PERGAMON

International Journal of Solids and Structures 38 (2001) 4657–4669

INTERNATIONAL JOURNAL OF SOLIDS and STRUCTURES

www.elsevier.com/locate/ijsolstr

Effects of a prestress on a reinforced, nonlinearly elastic and compressible tube subjected to combined deformations

M. Zidi *

Laboratoire de Mécanique Physique / ESA CNRS 7052, Faculté des Sciences et Technologie, Université Paris Val de Marne, 61, avenue du général De Gaulle, 94010 Créteil cédex, France

Received 10 December 1999; in revised form 26 July 2000

Abstract

We consider a nonlinearly elastic and prestressed tube subjected to a combined torsion and circular and axial shearing. The hollow cylinder's inner and outer surfaces are allowed to rotate by the torsion and the circular shear, and to displace in the longitudinal direction by the axial shear but not move radially. The analysis is carried out for a class of Blatz–Ko response augmented with unidirectional reinforcing that is characterized by a single additional constitutive parameter for strength of reinforcement. The form of solution sought leads to a system of nonlinear equations which are solved numerically. For different transverse isotropic materials, we show the effects of the prestress on the local volume change, the circumferential stretch ratio and the stress distributions.

1. Introduction

In recent years, there has been a considerable amount of interest in the study of finite compressible elasticity problems. Note that the mathematical formulations for compressible materials is considerably more complicated than incompressible cases. Indeed, the research on compressible, hyperelastic solids is relatively new and the scope of these works is more restricted due to the fact that the only controllable deformations are homogeneous deformations as was proved by Ericksen (1955). To put it more precisely, Ericksen has shown that the only deformations that can be sustained by every homogeneous, isotropic, elastic and compressible solid without body force are homogeneous deformations. As a consequence of these limitations, there are few exact solutions available within the context of compressible nonlinear constitutive theories in elasticity. Ogden and Isherwood (1978) have presented the solution of some finite plane-strain problems for compressible, isotropic elastic solids by using a direct method, which does not employ inverse or semi-inverse technique. Carroll and Horgan (1990) have also proposed several closed form finite strain equilibrium solutions for the Blatz–Ko constitutive law (Blatz and Ko, 1962; Beatty, 1987).

* Tel.: +33-1-4517-1442; fax: +33-1-4517-1433.
E-mail address: zidi@univ-paris12.fr (M. Zidi).

0020-7683/01/$ - see front matter
PII: S0020-7683(00)00308-5

The Blatz–Ko model is perhaps the most widely known constitutive model for compressible isotropic nonlinearly elastic solids. Its mathematical formulation characterizes the constitutive behavior of certain solid or foam rubber-like materials and was proposed on the basis of experiments carried out by them. Thus, Carroll and Horgan (1990) obtained solutions by the semi-inverse method, each of the deformations being a nonisochoric generalization of a deformation which is controllable for homogeneous, isotropic, incompressible elastic solids. The problems of finite deformations of compressible, isotropic, hyperelastic, long circular cylindrical tubes subjected to circular or axial shearing force on its outer curved surface have been extensively studied by various authors (Mioduchowski and Haddow, 1974; Ertepinar and Erarslanoglu, 1990; Ertepinar, 1990; Polignone and Horgan, 1992; Simmonds and Warne, 1992; Polignone and Horgan, 1994; Wineman and Waldron, 1995; Beatty and Jiang, 1995; Beatty and Jiang, 1997; Jiang and Ogden, 1998; Jiang and Ogden, 2000). Similarly, the torsion of a hyperelastic and isotropic hollow cylinder subjected to twisting moments at its ends has been a subject of attention (Levinson, 1972; Carroll and Horgan, 1990; Polignone and Horgan, 1991).

It must be emphasized that few studies include the combined deformations in the compressible case and the author is unaware of any published exact solution in this situation. Recently, there has been a resurgence of interest in determining solutions within the context of specific combined problems which are complicated to obtain, even in the isotropic case and for simple geometries. In the incompressible case, Tao et al. (1992) have considered a tube subjected to torsion and azimuthal shearing for generalized power-law neo-Hookean materials. They have shown that for certain values of the power-law exponent, exact solutions may be found. Mioduchowski and Haddow (1979) have studied a compressible hyperelastic cylinder subjected to finite circular and axial shear. A numerical solution has been obtained for two strain energy functions, those proposed by Levinson and Burgess (1971) and by Blatz and Ko (1962). The approximate solution is discussed in which the cylinder is divided into a number of coaxial thin-walled tubes of equal undeformed wall thickness. Distributions on the stresses and the radial stretch ratio of the current thickness to the undeformed wall thickness were obtained. More recently, Zidi (2000a) has discussed the deformation of a sector of a cylinder of a compressible hyperelastic material using a generalized Blatz–Ko constitutive equation. First, the deformation is considered which closes the sector, and then it is subjected to azimuthal shear and torsion. In this combined problem, the three equilibrium equations are transformed into a system of two ordinary differential equations for radial variation of the circumferential stretch ratio and the local volume change. Because no closed form solution seems possible, these coupled equations have been solved numerically. Soon after, using the same approach, the combined torsion and finite axial shear problem for a hollow cylinder was studied (Zidi, 2000b).

The purpose of the present paper is to extend one of these previous studies (Zidi, 2000a). For one, the tube is considered transversely isotropic and made of a Blatz–Ko reinforced material (Kurashige, 1981; Triantaffyllidis and Abeyaratne, 1983; Qiu and Pence, 1997; Zidi, 2000b). Note that the transverse isotropy considered can be interpreted as unidimensional fibers that are arranged and embedded in an isotropic matrix, the whole forming an anisotropic material (Spencer, 1984). For another, the tube is considered as prestressed and to be subjected to a deformation consisting of combined torsion and circular and axial shearing. Thus, as in previous works (Wineman and Waldron, 1995; Zidi, 2000a,b), the differential equations governing this new problem are explicitly obtained and solved numerically. As illustrative examples, we study the effects of different orientations of the fibers and we show clearly that an increase of the prestress modifies the results, particularly the gradient of the stress distributions in the tube.

2. Preliminaries

Consider a nonlinearly elastic body in its undeformed configuration. With respect to a cartesian coordinate system, let $\mathbf{X}$ and $\mathbf{x}$ denote, respectively, the position vector of a particle in the undeformed and the

deformed configuration. The components of the deformation gradient $\mathbf{F}$, the right Cauchy–Green deformation tensor $\mathbf{B}$ and the left Cauchy–Green deformation tensor $\mathbf{C}$ will be, respectively, denoted by

$$\mathbf{F} = \partial\mathbf{x}/\partial\mathbf{X}, \qquad \mathbf{B} = \mathbf{F}\overline{\mathbf{F}}, \qquad \mathbf{C} = \overline{\mathbf{F}}\mathbf{F}, \tag{1}$$

where $\overline{\mathbf{F}}$ is the transpose of $\mathbf{F}$.

Suppose that the material of the body is transversely isotropic, i.e. reinforced by "fibers" (Spencer, 1984). The corresponding elastic potential W depends on five strain invariants I_1, I_2, I_3, I_4 and I_5 expressed as

$$I_1 = \mathrm{tr}\mathbf{B}, \quad I_2 = \mathrm{tr}\mathbf{B}^*, \quad I_3 = J^2 = \det\mathbf{B}, \quad I_4 = \mathbf{T}.\mathbf{C}.\mathbf{T}, \quad I_5 = \mathbf{T}.\mathbf{C}^2.\mathbf{T}, \tag{2}$$

with $\mathbf{B}^* = (\det\mathbf{B})\mathbf{B}^{-1}$ is the adjoint of $\mathbf{B}$, J is the local volume change and $\mathbf{T} = (T_i)$ is the preferential direction vector in the undeformed configuration related to the transverse isotropic direction $\mathbf{t} = (t_i)$ in the deformed configuration by

$$\mathbf{t} = \frac{1}{\sqrt{I_4}}\mathbf{F}\mathbf{T}. \tag{3}$$

The corresponding response equation for the Cauchy stress tensor $\boldsymbol{\sigma}$ is

$$\boldsymbol{\sigma} = 2I_3^{-(1/2)}[(I_2W_2 + I_3W_3)\mathbf{1} + W_1\mathbf{B} - I_3W_2\mathbf{B}^{-1} + I_4W_4\mathbf{t}\otimes\mathbf{t} + I_4W_5(\mathbf{t}\otimes\mathbf{B}\mathbf{t} + \mathbf{t}\mathbf{B}\otimes\mathbf{t})], \tag{4}$$

where $\mathbf{1}$ is the identity tensor and $W_j = (\partial W/\partial I_j)$ $(j = 1,2,3,4,5)$.

Consider now a Blatz–Ko material reinforced in the $\mathbf{T}$ direction and take

$$W = \frac{\mu_0}{2}\left[(I_1 - 3) - \frac{2}{q}\left(I_3^{(q/2)} - 1\right) + k(I_4 - 1)^n\right], \tag{5}$$

where $q = (-2v_0/1 - 2v_0)$, and the scalars μ_0, v_0, respectively, are the usual constant shear modulus and Poisson's ratio for infinitesimal deformations from the undeformed configuration. The constants k and n represent, respectively, the density of reinforcement and the fiber stiffness.

Note that the isotropic case $k = 0$ characterizes the class of solid polyurethane rubbers (Blatz and Ko, 1962; Beatty, 1987) and when $I_3 \to 1$ (5) may be viewed as a compressible generalization of the reinforced neo-Hookean incompressible material (Qiu and Pence, 1997; Zidi et al., 1999).

Eqs. (4) and (5) yield the corresponding law expressed as

$$\boldsymbol{\sigma} = \mu_0\left[-J^{q-1}\mathbf{1} + \frac{1}{J}\mathbf{B} + kn\frac{I_4}{J}(I_4 - 1)^{n-1}\mathbf{t}\otimes\mathbf{t}\right]. \tag{6}$$

To motivate our particular choice of material defined by Eq. (5), we examine a state of plane-strain uniaxial stress parallel to the x_1-axis, $\sigma_{11} = F$, $\sigma_{22} = 0$, $\lambda_3 = 1$.

When the fibers are parallel to the direction of loading (i.e. $T_1 = 1$, $T_2 = 0$, $T_3 = 0$), it easily follows that from Eqs. (2) and (6) the applied stress F and the transverse stretch λ_2 are related to the principal stretch $\lambda_1 = \alpha$ as follows:

$$\frac{F}{\mu_0} = -\alpha^{\frac{2(1-q)}{q-2}} + \alpha^{\frac{2(q-1)}{q-2}} + \alpha^{\frac{2(q-1)}{q-2}}kn(\alpha^2 - 1)^{n-1}, \quad \lambda_2 = \alpha^{\frac{q}{2-q}}. \tag{7}$$

For the purposes of comparison, now consider normal fibers to the direction of loading (i.e. $T_1 = 0, T_2 = 1, T_3 = 0$), we obtain

$$\frac{F}{\mu_0} = -\alpha^{q-1} + \frac{\alpha}{\lambda_2}, \qquad \alpha = \lambda_2^{\frac{2-q}{q}}\left[1 + kn(\lambda_2^2 - 1)^{n-1}\right]^{\frac{1}{q}}. \tag{8}$$

As an illustration, Fig. 1 shows the stress–stretch relation F versus α for $k = 2.5$, $n = 2$ and the comparison with the isotropic case ($k = 0$). We show clearly that in tension the reinforcement has an effect on

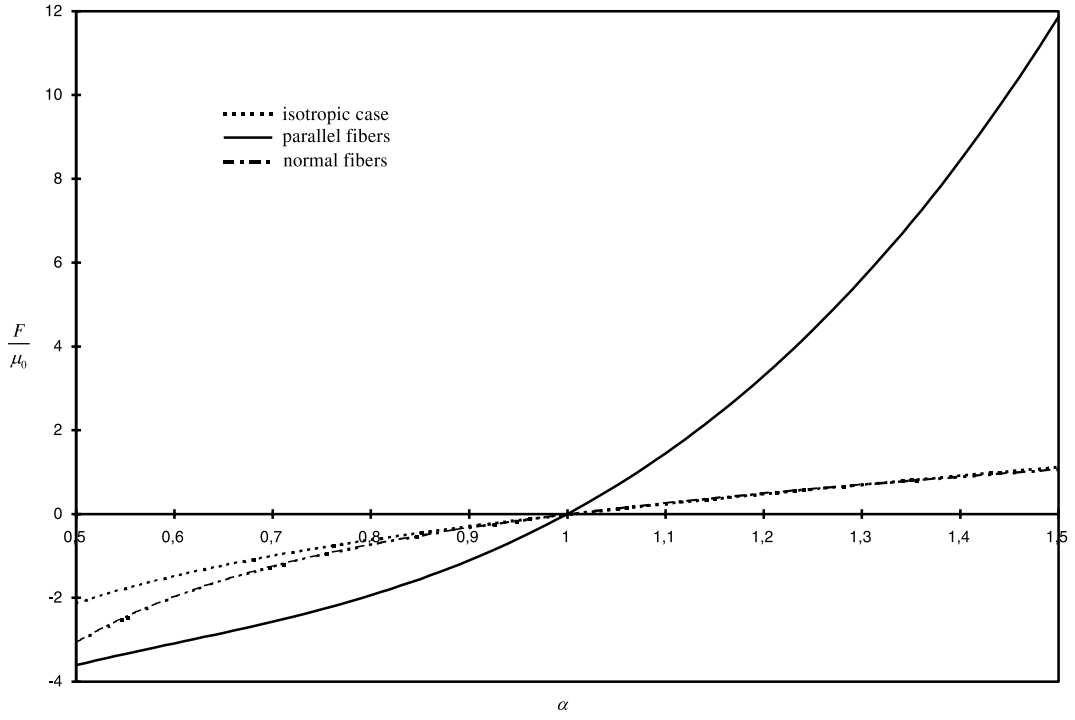

Fig. 1. Mechanical response of Blatz–Ko reinforced material in plane uniaxial stress. Stress versus stretch.

the mechanical behavior when fibers are aligned with the direction of the loading, whereas it has no effect when aligned in a direction normal to it. It must be emphasized that these results are comparable to those presented by Triantafyllidis and Abeyaratne (1983), when the reinforcement of the special Blatz–Ko material is considered.

3. Hollow cylinder subjected to combined deformation: formulation of boundary-value problem

We are now concerned with a sector of a circular and hollow cylinder composed of a material described by Eq. (5). The sector is defined by the angle Θ_0 (Fig. 2). Let us suppose that the tube undergoes two

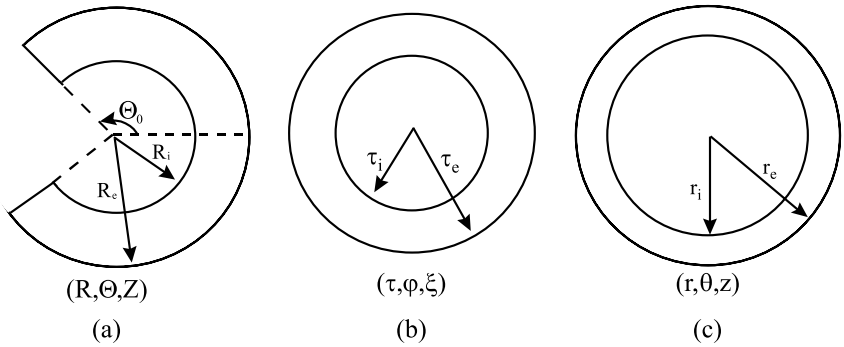

Fig. 2. Cross-section of the tube in (a) stress-free, (b) unloaded, and (c) loaded configuration.

successive deformations. First, the cylinder is closed, which induces a prestress (Sensenig, 1965; Zidi, 2000a), and then it is subjected to torsion, circular and axial shear. The mapping is described by

$$r = r(R), \qquad \theta = \left(\frac{\pi}{\Theta_0}\right)\Theta + \psi Z + \phi(r), \qquad z = Z + \omega(r), \tag{9}$$

where (R, Θ, Z) and (r, θ, z), respectively, are the reference and the deformed positions of a material particle in a cylindrical coordinate system. Here, ψ is a twist angle per unloaded length, ϕ is an angle which defines the circular shear and ω is an axial displacement which defines the axial shear. Let R_i and r_i denote, respectively, the inner surfaces of the cylinder in the reference state and in the deformed state (R_e and r_e are the outer surfaces). It follows from Eq. (9) that in terms of physical components, the deformation gradient $\mathbf{F}$ has the following representation in a cylindrical system

$$\mathbf{F} = \begin{bmatrix} \dot{r} & 0 & 0 \\ r\dot{r}\dot{\phi} & \frac{r}{R}\frac{\pi}{\Theta_0} & r\psi \\ \dot{r}\dot{\omega} & 0 & 1 \end{bmatrix} = \begin{bmatrix} \lambda_r & 0 & 0 \\ K_1\lambda_r & \frac{\lambda_\theta \pi}{\Theta_0} & r\psi \\ K_2\lambda_r & 0 & 1 \end{bmatrix}, \tag{10}$$

where the dot denotes the differentiation with respect to the argument, K_1, K_2, λ_r and λ_θ, respectively, denote the circular and the axial shear strains, and the radial and the circumferential stretch ratios.

Thus, the Cauchy–Green deformation tensors have the matrix representation

$$\mathbf{B} = \begin{bmatrix} \lambda_r^2 & K_1\lambda_r^2 & K_2\lambda_r^2 \\ K_1\lambda_r^2 & (K_1\lambda_r)^2 + (\lambda_\theta \frac{\pi}{\Theta_0})^2 + (r\psi)^2 & K_1K_2\lambda_r^2 + r\psi \\ K_2\lambda_r^2 & K_1K_2\lambda_r^2 + r\psi & (K_2\lambda_r)^2 + 1 \end{bmatrix}, \tag{11}$$

$$\mathbf{C} = \begin{bmatrix} \lambda_r^2(1 + K_1^2 + K_2^2) & K_1\lambda_r\lambda_\theta\frac{\pi}{\Theta_0} & K_1\lambda_r r\psi + K_2\lambda_r \\ K_1\lambda_r\lambda_\theta\frac{\pi}{\Theta_0} & (\frac{\lambda_\theta\pi}{\Theta_0})^2 & \frac{\lambda_\theta\pi}{\Theta_0}r\psi \\ K_1\lambda_r r\psi + K_2\lambda & \frac{\lambda_\theta\pi}{\Theta_0}r\psi & (r\psi)^2 + 1 \end{bmatrix}. \tag{12}$$

As in Section 2, consider a unidirectional reinforcement in the mechanical response of the tube.

Define $\overline{\boldsymbol{\sigma}} = (\boldsymbol{\sigma}/\mu_0)$, the normalized Cauchy stress tensor and examine a particular constant direction $\mathbf{T} = [0, T_\Theta, T_Z]$. Thus, from Eq. (3) we have $\mathbf{t} = [0, t_\theta, t_z]$, and using Eqs. (11) and (12), the nondimensional stress components from the constitutive equation (6) with respect to cylindrical coordinates are found to be

$$\begin{aligned}
\overline{\sigma}_{rr} &= -J^{q-1} + J\left(\frac{\Theta_0}{\lambda_\theta\pi}\right)^2, \\
\overline{\sigma}_{\theta\theta} &= -J^{q-1} + J\left(\frac{\Theta_0}{\lambda_\theta\pi}\right)^2 K_1^2 + \frac{1}{J}\left[\left(\frac{\lambda_\theta\pi}{\Theta_0}\right)^2 + (r\psi)^2\right] + \frac{kn}{J}I_4(I_4-1)^{n-1}t_\theta^2, \\
\overline{\sigma}_{zz} &= -J^{q-1} + J\left(\frac{\Theta_0}{\lambda_\theta\pi}\right)^2 K_2^2 + \frac{1}{J} + \frac{kn}{J}I_4(I_4-1)^{n-1}t_z^2, \\
\overline{\sigma}_{r\theta} &= J\left(\frac{\Theta_0}{\lambda_\theta\pi}\right)^2 K_1, \\
\overline{\sigma}_{\theta z} &= J\left(\frac{\Theta_0}{\lambda_\theta\pi}\right)^2 K_1K_2 + \frac{r\psi}{J} + \frac{kn}{J}I_4(I_4-1)^{n-1}t_\theta t_z, \\
\overline{\sigma}_{rz} &= J\left(\frac{\Theta_0}{\lambda_\theta\pi}\right)^2 K_2,
\end{aligned} \tag{13}$$

with $I_4 = (T_\Theta \lambda_\theta(\pi/\Theta_0))^2 + T_Z^2[(r\psi)^2 + 1] + 2T_\Theta T_Z r\psi\lambda_\theta(\pi/\Theta_0)$.

Furthermore, define $\overline{r} = r/R_\mathrm{i}$, $\overline{R} = R/R_\mathrm{i}$ and $\overline{z} = z/R_\mathrm{i}$ as nondimensional variables. Then, from Eq. (13), and upon ignoring the body force field, the equilibrium equations are reduced to

$$\frac{\mathrm{d}\overline{\sigma}_{rr}}{\mathrm{d}\overline{r}} + \frac{\overline{\sigma}_{rr} - \overline{\sigma}_{\theta\theta}}{\overline{r}} = 0, \tag{14}$$

$$\frac{\mathrm{d}\overline{\sigma}_{r\theta}}{\mathrm{d}\overline{r}} + \frac{2\overline{\sigma}_{r\theta}}{\overline{r}} = 0, \tag{15}$$

$$\frac{\mathrm{d}\overline{\sigma}_{rz}}{\mathrm{d}\overline{r}} + \frac{\overline{\sigma}_{rz}}{\overline{r}} = 0. \tag{16}$$

Note that Eqs. (15) and (16) can be solved for the circular and axial shear stress distribution

$$\overline{\sigma}_{r\theta} = \frac{\overline{F}_1}{\overline{r}^2}, \qquad \overline{\sigma}_{rz} = \frac{\overline{F}_2}{\overline{r}}, \tag{17}$$

where $\overline{F}_1$ and $\overline{F}_2$ are the nondimensional circular and axial shear force per unit length required to maintain the shear deformation. Then, from Eqs. (6) and (17) the expressions for the local shear strains K_1 and K_2 are

$$K_1 = \frac{\overline{F}_1\lambda_\theta^2}{\overline{r}^2 J}\left(\frac{\pi}{\Theta_0}\right)^2, \qquad K_2 = \frac{\overline{F}_2\lambda_\theta^2}{\overline{r}J}\left(\frac{\pi}{\Theta_0}\right)^2. \tag{18}$$

Thus, using equation $\lambda_r = (J/\lambda_\theta)(\Theta_0/\pi)$, obtained from the definition of the local volume change, and on substitution from Eq. (18), the normalized Cauchy stress tensor $\overline{\boldsymbol{\sigma}}$ can be written from $\overline{r}$, J and λ_θ, and the result is denoted by $\overline{\overline{\boldsymbol{\sigma}}}$. Then, from Eq. (14), we obtain a coupled system of nonlinear ordinary differential equations for $\lambda_\theta(\overline{r})$ and $J(\overline{r})$ which can be written as

$$\frac{\mathrm{d}\lambda_\theta}{\mathrm{d}\overline{r}} = \frac{\lambda_\theta}{\overline{r}}\left(1 - \frac{\lambda_\theta^2}{J}\frac{\pi}{\Theta_0}\right), \tag{19}$$

$$\frac{\mathrm{d}J}{\mathrm{d}\overline{r}} = \left(\frac{\mathrm{d}\overline{\overline{\sigma}}_{rr}}{\mathrm{d}\overline{r}} - \frac{\partial\overline{\overline{\sigma}}_{rr}}{\partial\overline{r}} - \frac{\partial\overline{\overline{\sigma}}_{rr}}{\partial\lambda_\theta}\frac{\mathrm{d}\lambda_\theta}{\mathrm{d}\overline{r}}\right)\left(\frac{\partial\overline{\overline{\sigma}}_{rr}}{\partial J}\right)^{-1}, \tag{20}$$

where

$$\frac{\mathrm{d}\overline{\overline{\sigma}}_{rr}}{\mathrm{d}\overline{r}} = \frac{1}{\overline{r}}\left[\frac{\lambda_\theta^2}{J}\left(\frac{\pi}{\Theta_0}\right)^2 - \frac{J}{\lambda_\theta^2}\left(\frac{\Theta_0}{\pi}\right)^2 + \frac{(\overline{r}R_\mathrm{i}\psi)^2}{J} + \frac{\overline{F}_1^2\lambda_\theta^2}{\overline{r}^4 J}\left(\frac{\pi}{\Theta_0}\right)^2 + \frac{kn}{J}t_\theta^2 I_4(I_4 - 1)\right], \tag{21}$$

$$\frac{\partial\overline{\overline{\sigma}}_{rr}}{\partial\overline{r}} = 0, \tag{22}$$

$$\frac{\partial\overline{\overline{\sigma}}_{rr}}{\partial\lambda_\theta} = -\frac{2J}{\lambda_\theta^3}\left(\frac{\Theta_0}{\lambda_\theta}\right)^2, \tag{23}$$

$$\frac{\partial\overline{\overline{\sigma}}_{rr}}{\partial J} = -(q-1)J^{q-2} + \left(\frac{\Theta_0}{\lambda_\theta\pi}\right)^2. \tag{24}$$

Let us consider the boundary conditions such as $r(R_i) = R_i$ and $r(R_e) = R_e$, which imply

$$\lambda_\theta(\bar{r}_i) = \lambda_\theta(\bar{r}_e) = 1, \tag{25}$$

where $\bar{r}_i = 1$ and $\bar{r}_e = R_e/R_i$. As a result, Eqs. (19) and (20) subject to the boundary conditions (25) form a boundary value problem for $\lambda_\theta(\bar{r})$ and $J(\bar{r})$, where $\overline{F}_1$ and $\overline{F}_2$ are fixed. Note that this approach has been used recently for other boundary value problems in the context of compressible finite elasticity (Wineman and Waldron, 1995; Zidi, 2000a,b).

On the other hand, we have derived the necessary and sufficient conditions on the strain energy function (5) for a pure deformation, with particular transverse isotropy directions. For that, pure torsion, pure circular shear or axial shear (Haughton, 1993; Wineman and Waldron, 1995; Zidi, 2000a) which correspond to $\lambda_r = \lambda_\theta = J = 1$ and $\Theta_0 = 180°$ are considered. Furthermore, we consider transverse isotropic direction as $\mathbf{T} = [0, T_\Theta, T_Z] = [0, \cos\gamma_0, \sin\gamma_0]$. Thus, the orientation of fibers is characterized by their tangent vector which depends on the given constant angle γ_0.

In this situation, examine the cases $\gamma_0 = 0°$, $\gamma_0 = 45°$ and $\gamma_0 = 90°$ which correspond, respectively, to circumferential, oriented at 45°, and axial fibers. For pure torsion ($\psi \neq 0$, $\overline{F}_1 = \overline{F}_2 = 0$), it follows from Eq. (18)

$$K_1 = K_2 = 0. \tag{26}$$

Then, from Eqs. (13) and (14) we obtain

$$(\bar{r}R_i\psi)^2 + kn\left\{T_\Theta^2 + T_Z^2[(\bar{r}R_i\psi)^2 + 1] + 2T_\Theta T_Z \bar{r}R_i\psi - 1\right\}^{n-1}(T_\Theta + \bar{r}R_i\psi T_Z)^2 = 0. \tag{27}$$

Thus, Eq. (27) does not hold verified for the fiber directions considered.

For pure circular shear ($\overline{F}_1 \neq 0$, $\overline{F}_2 = \psi = 0$), it follows from Eq. (18)

$$K_1 = \frac{\overline{F}_1}{\bar{r}^2}, \qquad K_2 = 0. \tag{28}$$

Then, from Eqs. (13) and (14) we obtain

$$\frac{\overline{F}_1}{\bar{r}^3} + knT_\Theta^2\left(T_\Theta^2 + T_Z^2 - 1\right)^{n-1} = 0. \tag{29}$$

Like the previous case, Eq. (29) does not hold.

For pure axial shear $\left(\overline{F}_1 = \psi = 0, \overline{F}_2 \neq 0\right)$, it follows from Eq. (18)

$$K_1 = 0, \qquad K_2 = \frac{\overline{F}_2}{\bar{r}}. \tag{30}$$

Then, from Eqs. (13) and (14) we obtain

$$knT_\Theta^2\left(T_\Theta^2 + T_Z^2 - 1\right)^{n-1} = 0. \tag{31}$$

This always holds, for fiber directions considered.

4. Numerical results and discussion

The effects of the prestress described in Section 3 are investigated. Note that the opening angle Θ_0 is a manifestation of the intensity of the prestress inside the tube, a decrease of Θ_0 being related to an increase in opening angle and intensity of the prestress (Sensenig, 1965; Zidi, 2000a). The variation of the stretch ratio, the volume ratio and nonzero stress components are presented by solving the nonlinear differential

equations (19) and (20). These equations are integrated numerically using the fourth order Runge–Kutta method with 51 points along the radial direction. The numerical method is also completed with an iterative process as in the paper of Wineman and Waldron (1995). Indeed, first, for given values of $\overline{F}_1$ and $\overline{F}_2$, $J(\overline{r}_i)$ is estimated. Using these values and the boundary condition $\lambda_\theta(\overline{r}_i) = 1$, Eqs. (19) and (20) are integrated for $\overline{r} = [\overline{r}_i, \overline{r}_e]$. The value of the circumferential stretch ratio was checked against the boundary condition $\lambda_\theta(\overline{r}_e) = 1$. Then, iterations are used to adjust the estimate for $J(\overline{r}_i)$ until the boundary condition $\lambda_\theta(\overline{r}_e) = 1$ is satisfied and the stress distributions are obtained. As an illustrative example, we take $\overline{r}_e = 2$ and $v_0 = 0.25$. We focus our attention on a case, where the torsion is neglected ($\psi = 0$) and when the tube is subjected to fixed circular and axial shear defined by $\overline{F}_1 = \overline{F}_2 = 2$.

To begin with, we consider the isotropic case ($k = 0$). Figs. 3 and 4 show the distribution of circumferential stretch ratio and the volume ratio. For each angle Θ_0, the material element volume is decreased ($J < 1$) at the inner support and increases with increasing $\overline{r}$. Near the outer shell, material element volume is increased ($J > 1$). At approximately $\overline{r} = 1.1$, material element volume is unchanged. Since $\lambda_\theta < 1$, the cylindrical surfaces move inward, which is consistent with the volume change as shown in Fig. 4. Also, it follows from Fig. 3 that the circumferential stretch ratio passes through a minimum. This minimum is smaller as Θ_0 is smaller (i.e. the prestress is greater). Clearly, in the outer surface, there is a pronounced effect on the local volume change when Θ_0 decreases. For the purpose of brevity, we have plotted only the nondimensional stress components $\overline{\sigma}_{\theta\theta}$ and $\overline{\sigma}_{zz}$. We show that an increase of the prestress has limited effects on the stress distributions in the outer surface (Figs. 5 and 6), while the stresses become significant in the inner surface. Thus, the stress gradient increases greatly with the prestress and becomes significant for the circumferential stress distributions (Fig. 5). Note that the results of the isotropic case are identical to those

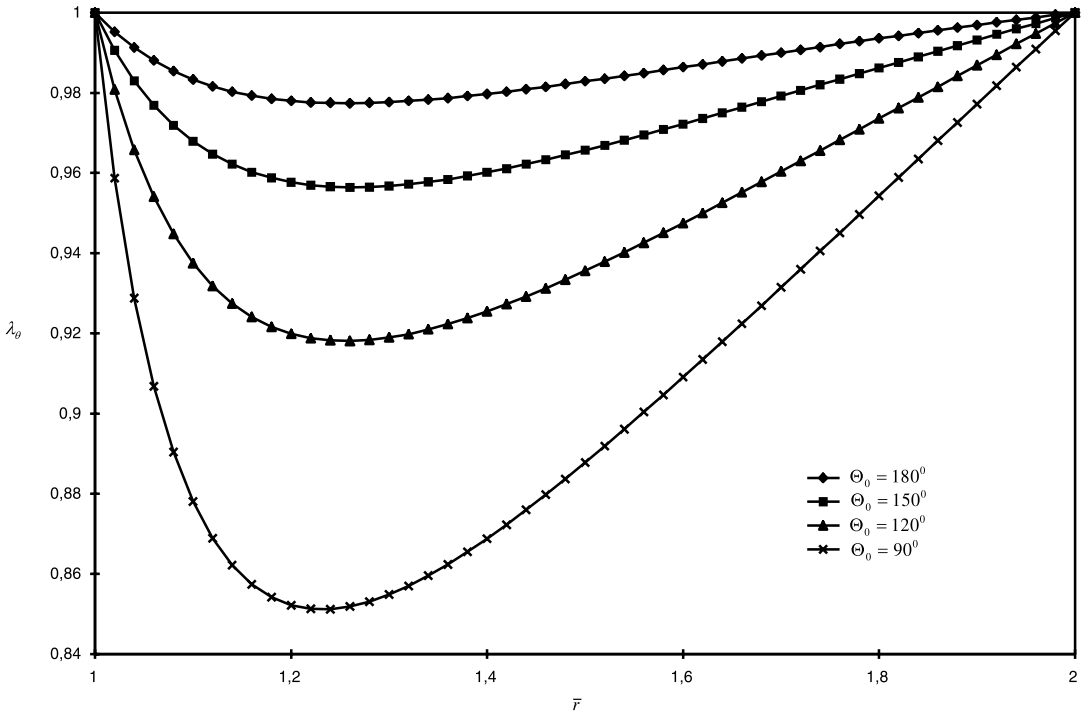

Fig. 3. Circumferential stretch ratio vs. radius for different values of Θ_0 ($k = 0$, $v_0 = 0.25$ and $\overline{F}_1 = \overline{F}_2 = 2$).

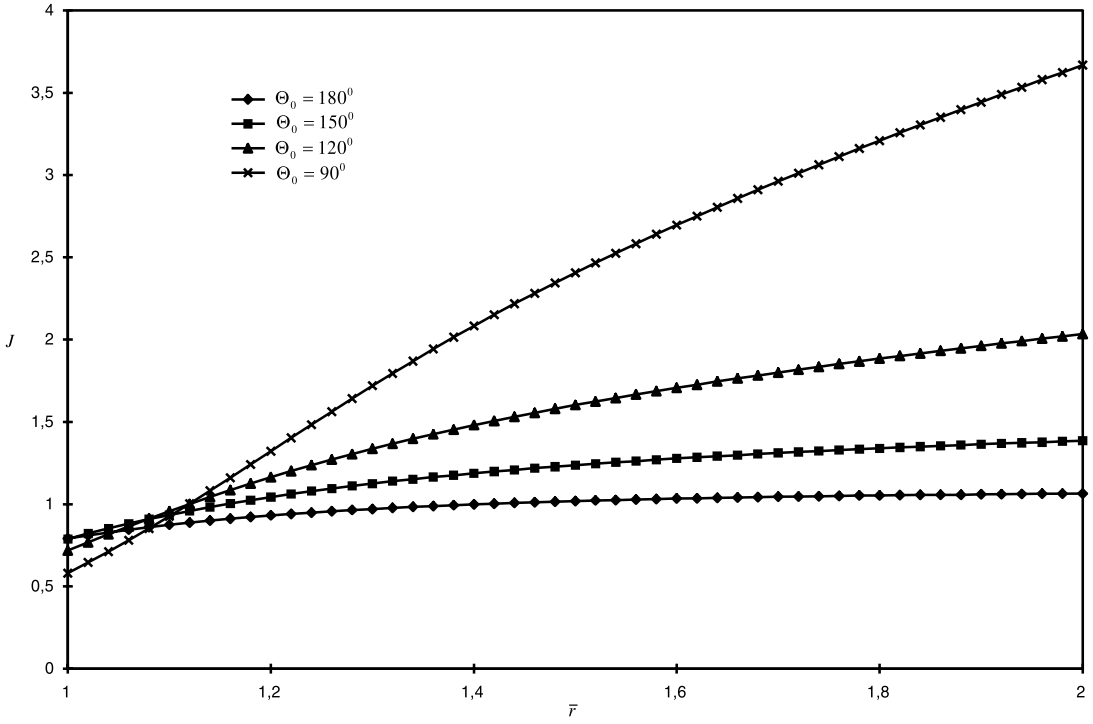

Fig. 4. Volume ratio vs. radius for different values of Θ_0 ($k = 0$, $v_0 = 0.25$ and $\overline{F}_1 = \overline{F}_2 = 2$).

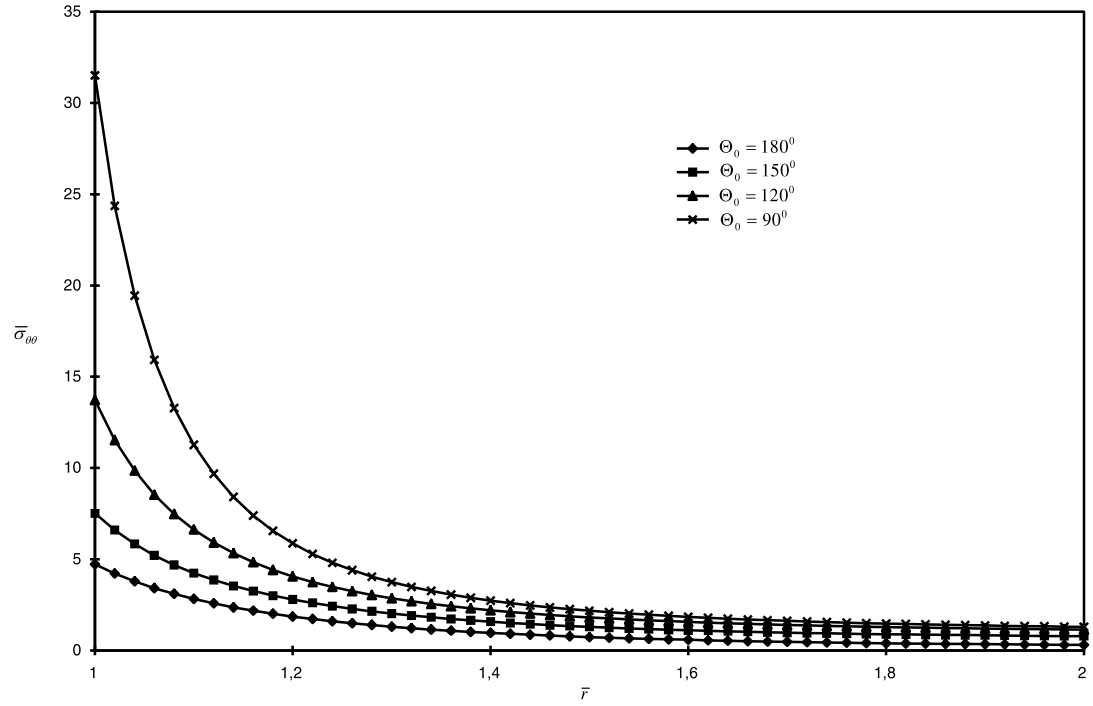

Fig. 5. Circumferential stress vs. radius for different values of Θ_0 $(v_0 = 0.25$ and $\overline{F}_1 = \overline{F}_2 = 2)$.

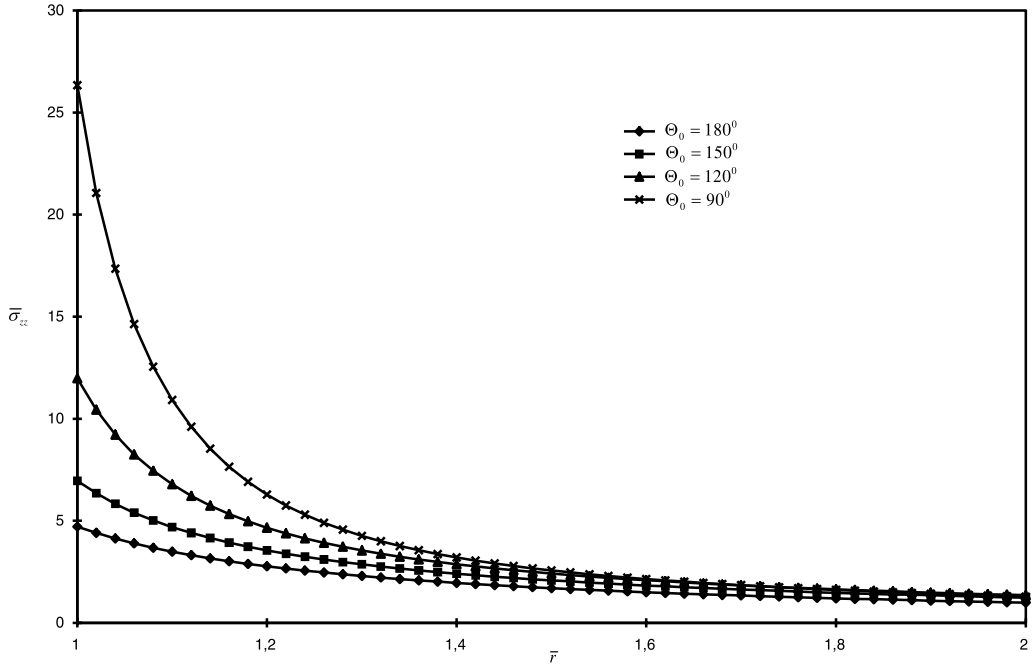

Fig. 6. Axial stress vs. radius for different values of Θ_0 $\left(\nu_0 = 0.25 \text{ and } \overline{F}_1 = \overline{F}_2 = 2\right)$.

of the transverse isotropic case with $\gamma_0 = 90°$ (axial fibers). Indeed, it easily follows from Eqs. (13) and (21) that the contribution of the fibers disappears.

For the purposes of comparison, we examine the transverse isotropic case for $k = 2.5$ and $n = 2$ with $\mathbf{T} = [0, \cos\gamma_0, \sin\gamma_0]$ (Section 3). An interesting example to study is the case $\gamma_0 = 0°$ (circumferential fibers). We observe that it is at approximately $\overline{r} = 1.2$ that the material element volume is unchanged. This is plotted in Fig. 8. When compared to the isotropic case, it must be emphasized that the material element volume is all the more unchanged near the inner surface as the angle γ_0 increases.

On the other hand, the specific transverse isotropy mentioned above ($\gamma_0 = 0°$) and the prestress contribute to disturb the distribution of J with greater intensities in the outer surface (Fig. 8) like that of the case $k = 0$. Note that relative to the isotropic case, the curve of the plots of the local volume change is different from the inner surface to the outer surface. Indeed, it is worthy of note that the examination of Fig. 8 shows that the curves are inverted compared to the isotropic case. Furthermore, the maxima are more important in the outer surface when the prestress increases. Fig. 7 shows the circumferential stretch distributions which also pass through minima. However, these minima have intensities less significant compared to the case without fibers.

On the other hand, as shown in Figs. 9 and 10, the stress distributions are comparable to the isotropic case, but the intensities are greater in the inner surface, which increases the stress gradient. Particularly, the circumferential stress becomes extremely important in the inner surface when the prestress increases (Fig. 9). Finally, it must be emphasized that at any intermediate orientation of the fibers, one expects the response to lie somewhere between these two previous cases ($\gamma_0 = 0°$ and $\gamma_0 = 90°$ or isotropic case). Without going into further details of the parametric study, it is important to point out that the results reported here do not change significantly when varying the intensity of the shear forces $\overline{F}_1$ and $\overline{F}_2$.

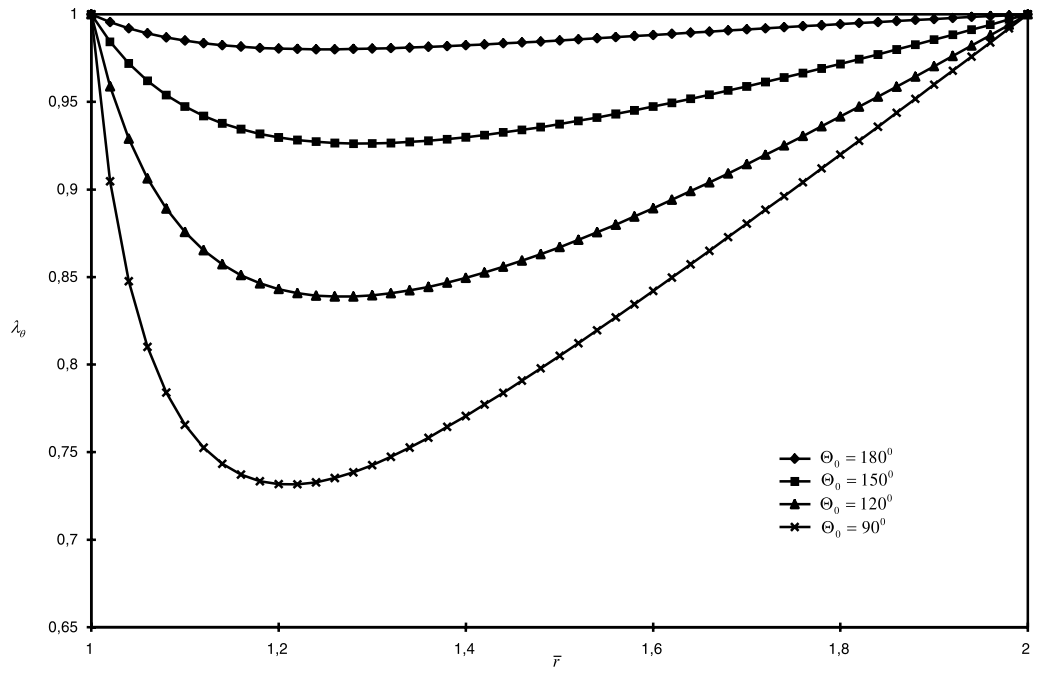

Fig. 7. Circumferential stretch ratio vs. radius for different values of Θ_0 ($\gamma_0 = 0°$, $k = 2.5$, $n = 2$, $v_0 = 0.25$ and $\overline{F}_1 = \overline{F}_2 = 2$).

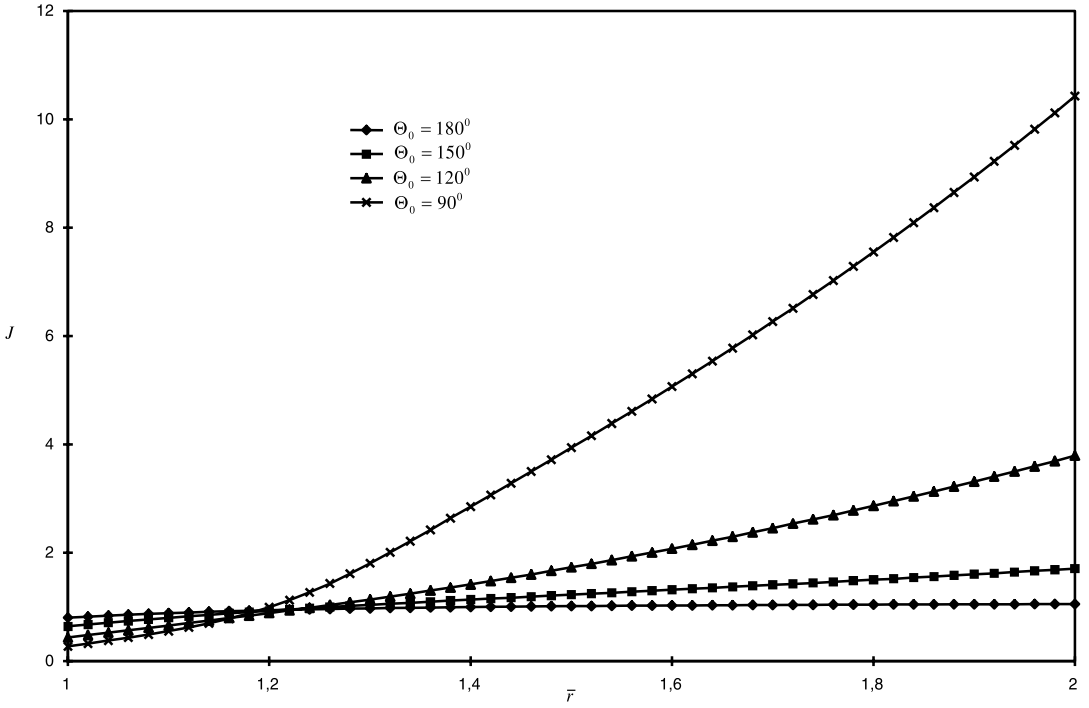

Fig. 8. Volume ratio vs. radius for different values of Θ_0 ($\gamma_0 = 0°$, $k = 2.5$, $n = 2$, $v_0 = 0.25$ and $\overline{F}_1 = \overline{F}_2 = 2$).

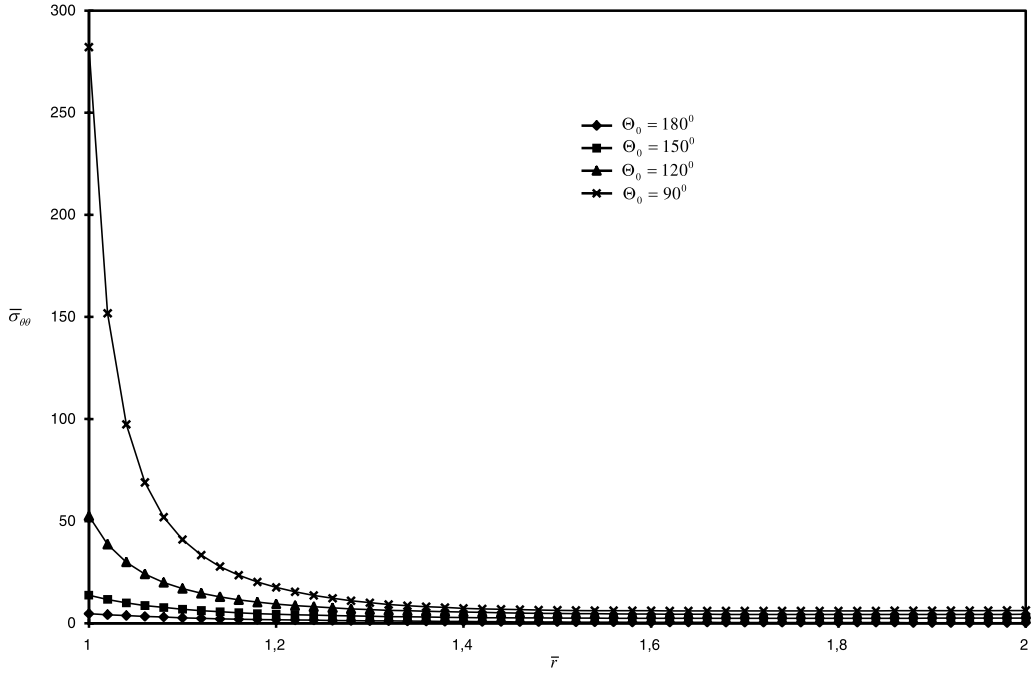

Fig. 9. Circumferential stress vs. radius for different values of Θ_0 ($\gamma_0 = 0°$, $k = 2.5$, $n = 2$, $v_0 = 0.25$ and $\overline{F}_1 = \overline{F}_2 = 2$).

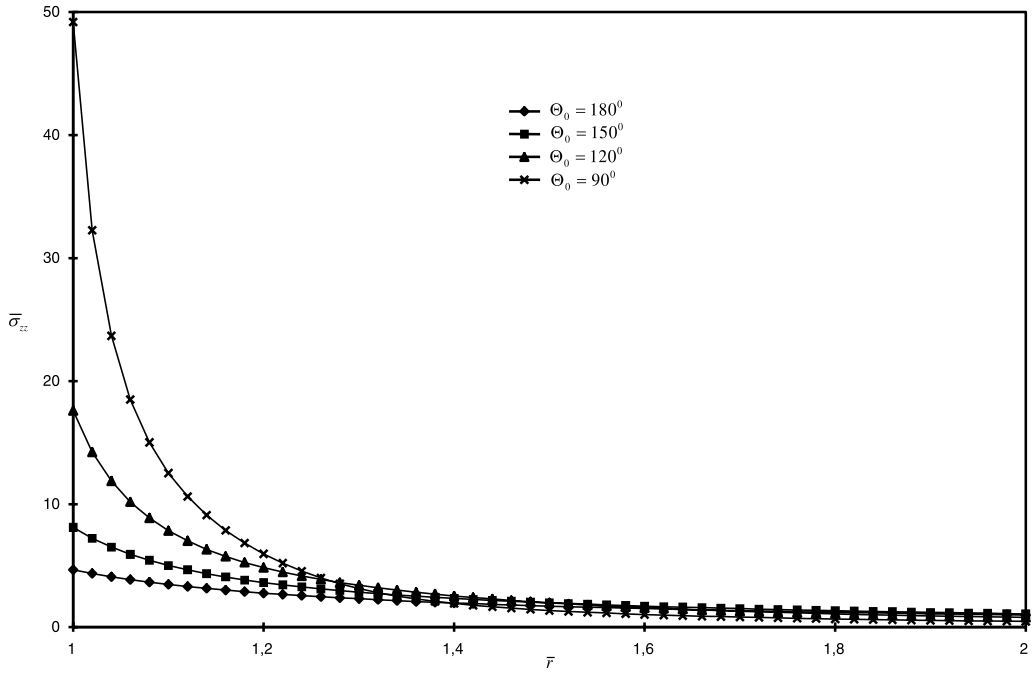

Fig. 10. Axial stress vs. radius for different values of Θ_0 ($\gamma_0 = 0°$, $k = 2.5$, $n = 2$, $v_0 = 0.25$ and $\overline{F}_1 = \overline{F}_2 = 2$).

References

Blatz, P.J., Ko, W.L., 1962. Application of finite elastic theory to the deformation of rubbery materials. Trans. Soc. Rheology 6, 223–251.

Beatty, M.F., 1987. Topics in finite elasticity: hyperelasticity of rubber, elastomers and biological tissues-with examples. Appl. Mech. Rev. 40, 1699–1734.

Beatty, M.F., Jiang, Q., 1995. On compressible materials capable of sustaining axisymmetric shear deformations. Part 1: Anti-plane shear of isotropic hyperelastic materials. J. Elasticity 39, 75–95.

Beatty, M.F., Jiang, Q., 1997. On compressible materials capable of sustaining axisymmetric shear deformations. Part 2: Rotational shear of isotropic hyperelastic materials. Quart. J. Mech. Appl. Math. 50, 211–237.

Carroll, M.M., Horgan, C.O., 1990. Finite strain solutions for a compressible elastic solid. Quart. Appl. Math. 48 (4), 767–780.

Ericksen, J.L., 1955. Deformations possible in every compressible isotropic, perfectly elastic material. J. Math. Phys. 34, 126–128.

Ertepinar, A., 1990. On the finite circumferential shearing of compressible hyperelastic tubes. Int. J. Engng. Sci. 28, 889–896.

Ertepinar, A., Erarslanoglu, G., 1990. Finite anti-plane shear of compressible hyperelastic tubes. Int. J. Engng. Sci. 28, 399–406.

Haughton, D.M., 1993. Shearing of compressible elastic cylinders. Quart. J. Mech. Appl. Math. 46, 471–486.

Jiang, X., Ogden, R.W., 1998. On azimuthal shear of a circular cylindrical tube of compressible elastic material. Quart. J. Mech. Appl. Math. 51, 143–158.

Jiang, X., Ogden, R.W., 2000. Some new solutions for the axial shear of a circular cylindrical tube of compressible elastic material. Int. J. Non-Linear Mech. 35, 361–369.

Kurashige, M., 1981. Instability of a transversely isotropic elastic slab subjected to axial loads. J. Appl. Mech. 48, 351–356.

Mioduchowski, A., Haddow, J.B., 1974. Finite telescopic shear of a compressible hyperelastic tube. Int. J. Non-Linear Mech. 9, 209–220.

Mioduchowski, A., Haddow, J.B., 1979. Combined torsional and telescopic shear of a compressible hyperelastic tube. J. Appl. Mech. 46, 223–226.

Levinson, M., Burgess, I.W., 1971. A comparison of some simple constitutive relations for slightly compressible rubber-like materials. Int. J. Mech. Sci. 13, 563–572.

Levinson, M., 1972. Finite torsion of slightly compressible rubberlike circular cylinders. Int. J. Non-Linear Mech. 7, 445–463.

Polignone, D.A., Horgan, C.O., 1991. Pure torsion of compressible non-linearly elastic circular cylinders. Quart. Appl. Math. 49 (3), 591–607.

Polignone, D.A., Horgan, C.O., 1992. Axisymmetric finite anti-plane shear of compressible non-linearly elastic circular tubes. Quart. Appl. Math. 50, 323–341.

Polignone, D.A., Horgan, C.O., 1994. Pure circular shear of compressible non-linearly elastic tubes. Quart. Appl. Math. 50, 113–131.

Ogden, R.W., Isherwood, D.A., 1978. Solution of some finite plane-strain problems for compressible elastic solids. Quart. J. Mech. Appl. Math. 31, 219–249.

Qiu, G.Y., Pence, T.J., 1997. Remarks on the behavior of simple directionally reinforced incompressible non-linearly elastic solids. J. Elasticity 49, 1–30.

Sensenig, C.B., 1965. Non-linear theory for the deformation of pre-stressed circular plates and ring. Commun. Pure Appl. Math. 18, 147–161.

Simmonds, J.G., Warne, P., 1992. Azimuthal shear of compressible or incompressible, non-linearly elastic polar orthotropic tubes of infinite extent. Int. J. Non-Linear Mech. 27, 447–467.

Spencer, A.J.M., 1984. Continuum theory of the mechanics of fibre-reinforced composites. Springer, Berlin.

Tao, L., Rajagopal, K.R., Wineman, A.S., 1992. Circular shearing and torsion of generalized neo-Hookean materials. IMA J. Appl. Math. 48, 23–37.

Triantafyllidis, N., Abeyaratne, R., 1983. Instability of finitely deformed fiber-reinforced elastic material. J. Appl. Mech. 50, 149–156.

Wineman, A.S., Waldron Jr., W.K., 1995. Normal stress effects induced during circular shear of a compressible non-linear elastic cylinder. Int. J. Non-Linear Mech. 30 (3), 323–339.

Zidi, M., Cheref, M., Oddou, C., 1999. Finite elasticity modelling of vascular prostheses mechanics. Eur. Phys. J. Appl. Phys. 7 (3), 271–275.

Zidi, M., 2000a. Circular shearing and torsion of a compressible hyperelastic and prestressed tube. Int. J. Non-Linear Mech. 35, 201–209.

Zidi, M., 2000b. Finite torsion and anti-plane shear of a compressible hyperelastic and transversely isotropic tube. Int. J. Engng. Sci. 38 (13), 1487–1496.